This is a preprint of the paper entitled ”Grüneisen parameter formalism in the study of the Earth’s core formation: a sensitivity study” by Vincent Clesi and Renaud Deguen. This version is the version that has been reviewed and accepted for publication in the journal Geophysical Journal International in March 2024. The proof reading and editing has not been done yet

submitted to *Geophys. J. Int.*

Grüneisen parameter formalism in the study of the Earth's core formation: a sensitivity study

Vincent Clesi[1,2] and Renaud Deguen[3,1]

[1] *Univ Lyon, ENSL, UCBL, UJM, CNRS, LGL-TPE, F-69007 Lyon, France*

[2] *Rice University Department of Earth Science. Keith-Wiess Geological Laboratory. 6100 Main Street Houston*

[3] *Univ. Grenoble Alpes, Univ. Savoie Mont Blanc, CNRS, IRD, Univ. Gustave Eiffel, ISTerre, 38000 Grenoble, France*

SUMMARY

The Grüneisen parameter is an important parameter for the thermal state and evolution of the core, but its uncertainties and their implications are sometimes overlooked . Several formalisms using different parameters values have been used in different studies, making comparison between studies difficult. In this paper, we use previously published datasets to test the sensitivity of modeling the thermal state of the early core to the different formalisms and parameter values used to describe the evolution of the Grüneisen parameter with density. The temperature of the core obtained in our models is less sensitive to the uncertainties of the parameters used in Al'Tshuler et al. (1987) formalism than the uncertainties of the parameters used in Anderson (1967) formalism.

Key words: Composition and structure of the core – Planetary interiors – Numerical modelling – High-pressure behaviour– Equations of state.

1 INTRODUCTION

Constraining the core heat content, whether at the present time (Lin et al. 2003; Labrosse 2015) or for the primitive core (Clesi & Deguen 2023), implies making assumptions on the thermal expansion and compressibility of the core components. For this, the Grüneisen parameter (first defined in Grüneisen 1912) is often used. This parameter has the advantage of being comprised between 0.9 and 2 for metallic materials, which is a narrower range than the thermal expansion coefficient or bulk modulus, and its value has been determined by different methods : thermodynamical modeling (Anderson 1967; Al'Tshuler et al. 1987), ab initio (Dubrovinsky et al. 2000; Alfè et al. 2007), experiments (Jeanloz 1979; Umemoto & Hirose 2015). Using the Grüneisen parameter allows to simplify the models by getting rid of the thermal expansion parameter α which is more sensitive to the composition.

However, there are several approaches to model the variations of the Grüneisen parameter, especially with pressure. Some studies assume a constant value (Anderson & Ahrens 1994; Labrosse 2015), some use the Al'Tshulher formalism (Al'Tshuler et al. 1987; Dewaele et al. 2006; Umemoto & Hirose 2015), some use the power law first proposed by Anderson in 1967 (Anderson 1967; Dubrovinsky et al. 2000; Kuwayama et al. 2020), while others calculate it within the study: by ab initio in Alfè et al. (2007) and Ichikawa et al. (2014), by linear expansion in Badro et al. (2014). In this paper, we will use the results of our previous study (Clesi & Deguen 2023) to assess the model sensitivity to different approaches of Grüneisen parameter when modeling the initial heat content of the core. We use previous results linking core composition and temperature, and test different ways of calculating the value of γ. By fitting the effect of each parameter on temperature, we can assess the variations introduced by using different formalisms, and the error introduced by variations of the parameters within the formalism chosen. We show that the formalism of Al'Tshuler (Al'Tshuler et al. 1987) is less prone to yield large errors in the calculations while being theoretically the most sound of all formalism studied.

2 GRÜNEISEN PARAMETER MODELING AND THERMAL MODEL

2.1 Accretion scenario and thermal modeling

We use the accretion and core/mantle differentiation models that have been previously determined in Clesi & Deguen (2023). These models yield mantle compositions close to the Bulk Silicate Earth (BSE) given in McDonough & Sun (1995), while yielding compositions for the core compatible with a $\sim 10\%$ wt. of light elements (Si and O) in the core. To determine the heat content and temperature of the core we consider the following steps :

(i) The initial temperature of each addition of metal is set at the bottom of the magma ocean, where the metal is assumed to equillibrate with the silicates. The initial temperature is therefore given by the liquidus of silicate at the pressure of the bottom of the magma ocean, as given by Andrault et al. (2011).

(ii) The metal is then heated by compression while migrating from the bottom of the magma ocean to the growing core. At each step of accretion its composition is different, and we do not consider any mixing, thus resulting in the formation of a stratified core (as in Jacobson et al. (2017))

(iii) The initial temperature profile is then set by the additional compression of the metal up to the final core pressures. We use this initial temperature and density profile to calculate the heat content.

(iv) We assume that the core is then mixed from the stratified state to an isentropic state, and use the previously calculated heat content to get the corresponding temperature at the CMB (T^{is}_{CMB}). This is a strong assumption, since the core is often found to be stably stratified at the end of accretion (Clesi & Deguen 2023). Whether the core would be efficiently mixed depends on the radial variations in composition, ratio of temperature gradient to isentropic gradient (which depends on γ), and of the nature and intensity of the possible stirring processes (Jacobson et al. 2017; Bouffard et al. 2020). However, the main purpose of this assumption is to provide a single measure of the temperature of the core – the temperature T^{is}_{CMB} of the CMB after mixing to an isentropic state – which can be seen as a convenient measure of the amount of heat stored into the core.

The details on the model and the different calculations are described in Clesi & Deguen (2023). The main result of the paper is that mean pressure of metal-silicate equilibrium, light elements concentration in the core, and core temperature are positively correlated. A summary of the results are presented in Figure 1.

The initial temperature of the metal is set to be the liquidus temperature of the silicate (Andrault

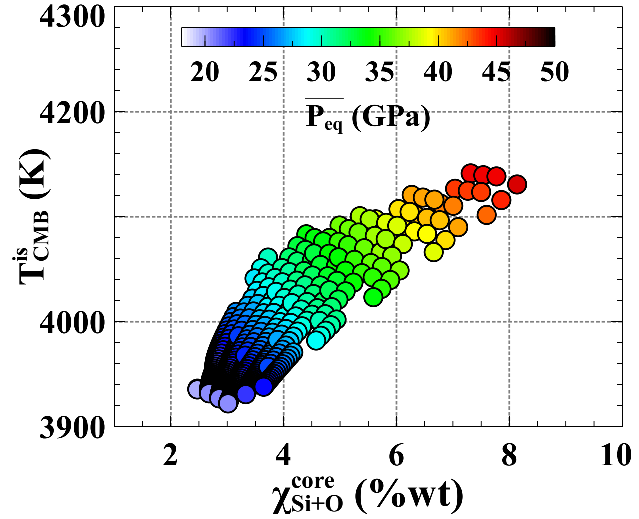

Figure 1. Summary of the results from Clesi & Deguen (2023), showing the correlation between the isentropic temperature at the CMB at the end of accretion (y-axis), light elements concentration in the core (here Si and O, x-axis) and mean value of equilibrium pressure ($\overline{P_{eq}}$, color scale). The temperatures obtained here are obtained with the Grüneisen parameter calculated with Al'Tshuler formalism, with $\gamma_0 = 1.875$ and $\gamma_\infty = 1.305$. The points plotted here are the models matching the compositional constraints defined in Clesi & Deguen (2023).

et al. 2011) at the bottom of the magma ocean where chemical equilibrium happens. It is given by:

$$T_{eq} = 1940 \left(\frac{P_{eq}}{29} + 1 \right)^{1/1.9}. \tag{1}$$

where P_{eq} is the pressure at the bottom of the magma ocean (in GPa) which is the pressure where metal and silicate are equilibrated. The temperature changes calculated in steps (ii) and (iii) are obtained from:

$$\frac{dT}{dP} = \frac{\gamma T}{K_s}. \tag{2}$$

where γ is the Grüneisen parameter of the metal, T its temperature and K_s its isentropic bulk modulus. We use the Murnaghan approximation for the bulk modulus,

$$K_s = K_0 + K'P, \tag{3}$$

with $K_0 = 128.49$ GPa the bulk modulus for P=0, and $K' = 3.67$ the first derivative of the bulk modulus, which yields the following equation of state for the metal:

$$\frac{\rho(P)}{\rho_0} = \left(1 + \frac{K'}{K_0} P \right)^{1/K'}. \tag{4}$$

with $\rho(P)$ is the density of the metal at pressure P. The value of ρ_0, i.e. the density of the metal at the reference pressure, is varying throughout accretion, depending on the composition of the metal, which is set by chemical equilibration with the silicates at the bottom of the magma ocean (see Clesi & Deguen (2023) for the details).

The heat content of the core is then calculated as

$$Q = 4\pi \int_0^{R_c} \rho(r) C_p T(r) r^2 dr, \tag{5}$$

with $R_C = 3470$ km the total radius of the core, $C_p = 1000 J.kg^{-1}.K^{-1}$ the specific heat of the metal and $T(r)$ the temperature in the core at the radius r; where the distance r from the center and the pressure are linked by

$$P_{core}(r) = P_{center} + \left(\frac{P_{CMB} - P_{center}}{R_c^2} \right) r^2 \tag{6}$$

with P_{CMB} and P_{center} the pressure at the CMB and at the center of the core, respectively. The isentropic temperature profile can then be obtained from

$$\left(\frac{\partial \ln T^{is}}{\partial \ln \rho^{is}} \right)_s = \gamma. \tag{7}$$

where ρ^{is} is the density profile of the core after isentropic mixing. As seen in Equation 7, the final isentropic temperature is a function of the Grüneisen parameter, γ. Depending on the γ formalism (constant value, Al'Tshuler et al. (1987) or Anderson (1967) power laws), integration of Equation 7 will yield different results. We then consider that the core is fully mixed with a constant heat content. The isentropic mixed core temperature profile is determined by integration of Equation 7 for a mixed density profile $\rho^{is}(r)$, and combined with the heat content calculated by Equation 5, we can calculate the temperature at the CMB after mixing as

$$T_{CMB}^{is} = \frac{Q}{4\pi \int_0^{R_c} \rho^{is}(r) C_p T^{is}(r) r^2 dr}, \tag{8}$$

which is evaluated numerically. In the following sections, we calculate T_{CMB}^{is} from equation 8 for the three different formalisms tested in this study, and we vary parameters values within each of the formalism to determine the sensitivity of T_{CMB}^{is} to the formalisms and parameter values. Before varying the parameters, Figure 2 shows how, for three solutions in the dataset presented in Figure 1, changing the formalism affects each step of the calculation. As can be seen on this figure, changing the value of the Grüneisen parameter tends to shift the temperature profiles up and down, irrespectively of the stratification.

2.2 Constant gruneisen parameter

The first assumption that can be made is assuming γ to be constant. Integration of Equation 2 then yields:

$$T(P) = T_{eq} \left(\frac{K'P + K_0}{K'P_{eq} + K_0} \right)^{\frac{\gamma}{K'}} . \tag{9}$$

This equation is used as input to calculate the heat content (Equation 5) and then the value of T_{CMB}^{is} (Equation 8).

2.3 Power law formalism of Anderson

The second assumption is that the variation of γ follows a power law of the form

$$\gamma = \gamma_0 \left(\frac{\rho_0}{\rho} \right)^b . \tag{10}$$

where γ_0 is the Grüneisen parameter for $\rho = \rho_0$ and b is the exponent of the power law. This formalism has been proposed by Anderson (1967), in order to simplify the calculation of the thermal expansion coefficient of some materials. This power law is practical for integration, and is especially fitted for Murnaghan equation of state, as it was one of the reasons for choosing this formalism in the original paper. Equation 2 with γ given by (10) has the following analytical solution:

$$T(P) = T_{eq} \exp \left[\frac{\gamma_0}{b} \left(\left(1 + \frac{K'P_{eq}}{K_0} \right)^{-b/K'} - \left(1 + \frac{K'P}{K_0} \right)^{-b/K'} \right) \right] . \tag{11}$$

2.4 Formalism of Al'Tshuler

The last model investigated in this study is given by

$$\gamma = \gamma_\infty + (\gamma_{0,j} - \gamma_\infty) \left(\frac{\rho_0}{\rho} \right)^\beta , \tag{12}$$

where $\beta = \gamma_{0,j}/(\gamma_{0,j} - \gamma_\infty)$, and $\gamma_{0,j}$ the Grüneisen parameter for $\rho = \rho_0$ and γ_∞ the asymptotic value of the Grüneisen parameter when $P \to \infty$. This equation also takes the form of a power

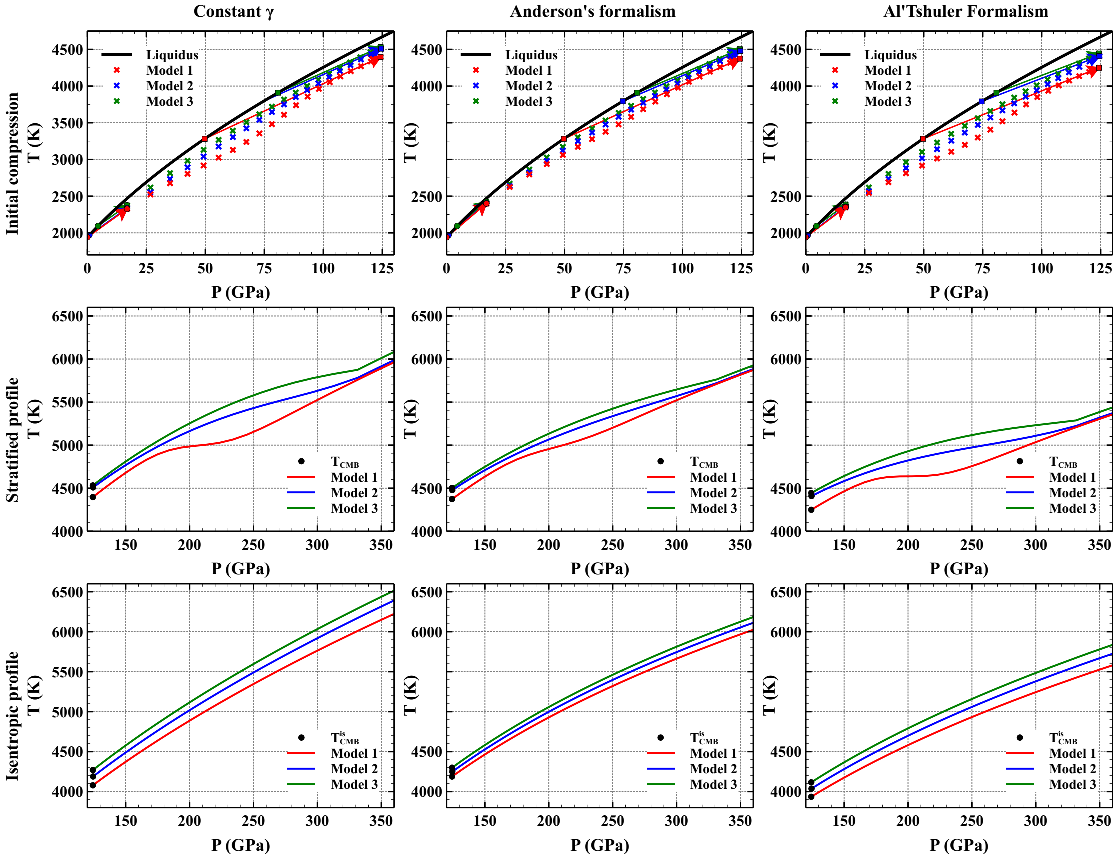

Figure 2. Description of three steps of the model for different formalisms of the Grüneisen parameter tested in this study. Left column: constant $\gamma = 1.7$. Middle column: Anderson's power law, with $\gamma_0 = 2.05$ and $b = 0.6$. Right column: Al'Tshuler formalism with $\gamma_0 = 1.305$ and $\gamma_\infty = 1.875$. Each row represents one of the steps of the scenario described in section 2.1. Top row: initial compression between the bottom of the magma ocean and the growing core-mantle boundary (step (i) and part of step (ii) in the text), with the liquidus curve in black and the adiabat of the first and last steps of the model shown by the arrows. The cross symbols represents the P-T conditions of the metal reaching the CMB at each step of accretion, before the core is fully formed. The arrows show the changes in P-T conditions undergone by the metal through the crystallized part of the mantle in the first step of accretion (round markers) and last step of accretion (square markers). Middle row: temperature profile of the core when stratified and after compression of the metal due to the growth of the core (step (ii) and step (iii) in the text). Bottom row: temperature profile in the core after mixing to an isentropic state (step (iv) in the text). The black dots mark the temperature at the CMB. A similar figure with more details on the model steps can be found at Clesi & Deguen (2023). Red curves: Model 1, obtained for the $f_c = 0.6$, $a_P = 0.4$ and $\lambda = 5$, with $\overline{P_{eq}} = 19.7$ GPa and $\chi^{core}_{Si+O} = 2.47\%$. Blue curves: Model 2, obtained for the $f_c = 0.85$, $a_P = 0.6$ and $\lambda = 1$, with $\overline{P_{eq}} = 34.1$ GPa and $\chi^{core}_{Si+O} = 5.24\%$. Green curves: Model 3, obtained for the $f_c = 1$, $a_P = 0.65$ and $\lambda = 0.4$, with $\overline{P_{eq}} = 43.9$ GPa and $\chi^{core}_{Si+O} = 7.86\%$.

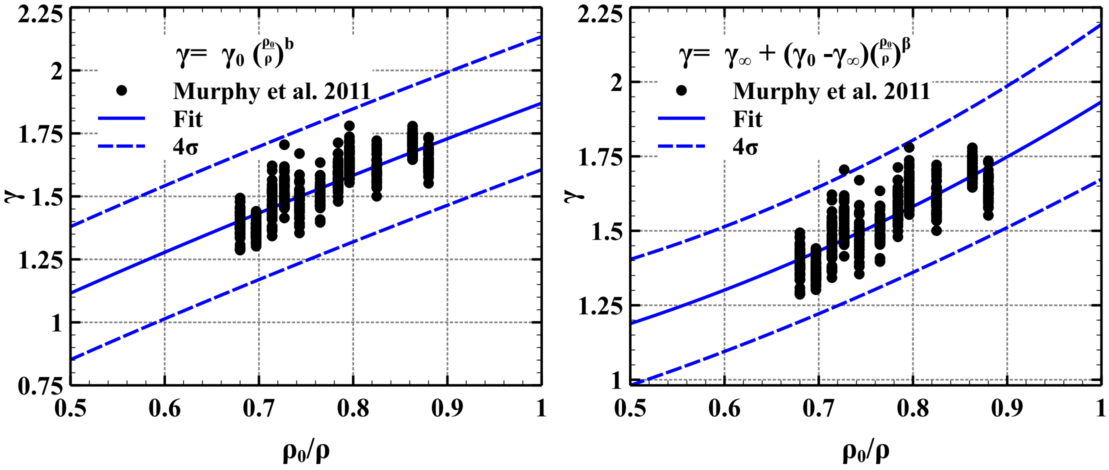

Figure 3. Results of the fit from the data of Murphy et al. (2011) with the formalism of Anderson (1967) (left panel) and Al'Tshuler et al. (1987) (right panel). The data from Murphy et al. (2011) have been bootstrapped to account for the error bar by randomly distributing 20 values for each point following a gaussian distribution, thus allowing the fit to be made on $\sim$ 200 points instead of 10.

law, used by multiple studies (Dewaele et al. 2006; Clesi & Deguen 2023). It is however different than the one from Anderson (1967), because it is derived from the theoretical isothermal density evolution of metal (Al'Tshuler et al. 1987). Though equation 12 might be seen as an extended version of Anderson's power law (it is the sum of a power law in ρ and a constant), note that the power exponent and the prefactor of the power law part are here linked theoretically, which is not the case in Anderson's power law. One implication is that the number of parameters involved in Al'Tshuler's formalism is not higher than in Anderson's formalism, in spite of its seamingly greater complexity. With this formalism, integrating equation 2 gives

$$T(P) = T_{eq}\left(\frac{K_0 + K'P}{K_0 + K'P_{eq}}\right)^{\frac{\gamma_\infty}{K'}} \times \exp\left[\frac{\gamma_{0,j} - \gamma_\infty}{\beta}\left(\left(1 + \frac{K'P_{eq}}{K_0}\right)^{-\frac{\beta}{K'}} - \left(1 + \frac{K'P}{K_0}\right)^{-\frac{\beta}{K'}}\right)\right]. \tag{13}$$

2.5 Sensitivities of T^{is}_{CMB} to the different parameters

In order to compare the three formalisms presented above, we fitted equations (10) and (12) to a dataset of Grüneisen parameter measurements for pure iron. This allows to obtain in a self-consistent way the values and uncertainties of the parameters appearing in Al'Tshuler et al. (1987) and Anderson (1967)'s formalisms. We use the dataset provided by Murphy et al. (2011), to which

Parameters	γ_0	b	$\gamma_{0,j}$	γ_∞
Mean value	1.875	0.752	1.933	0.916
Minimum value	1.555	0.432	1.608	0.591
Maximum value	2.195	1.07	2.258	1.241
1σ	0.08	0.08	0.0812	0.0812

Table 1. Values obtained from fitting the measurements of γ from Murphy et al. (2011) to the Anderson's and Al'Tshuler's formalisms.

we fitted the values of γ_0, b, γ_∞ and $\gamma_{0,j}$ (Figure 3). Given the limited number of points (10) in the dataset, we created for each value of $\frac{\rho_0}{\rho}$ a random dataset of 20 γ values distributed following a normal law centered on the mean value with a standard deviation equal to the uncertainty given in Murphy et al. (2011). We then fitted the parameters of each formalism to the dataset, thus allowing us to define a range of value for each parameter, given in Table 1, that will be tested throughout the study.

We use the subset of core formation models ($n = 382$) from Clesi & Deguen (2023). Each solution represents a different evolution of the core composition while yielding an acceptable fit on the Bulk Silicate Earth (McDonough & Sun 1995). We then calculate for each solution the CMB temperature after core mixing with equations 5 and 8 with the three different formalisms: equation 9 for constant γ, equation 10 for Anderson's power law, and equation 13 for Al'Tshuler's formalism. We vary each parameter independently to assess their effect on the mean and variance of T^{is}_{CMB} value on the 382 models tested. In the following sections we discuss the strengths and weaknesses of each formalism in the same style.

For each formalism, we estimate the effect of varying parameter values on the mean value of T^{is}_{CMB} in the dataset. In order to estimate the sensitivity of the model results to the parameters, we fitted a linear equation to explain the mean T^{CMB}_{is} value of our dataset:

$$T^{is}_{CMB} = a_0 + a_1 x \tag{14}$$

where x is one of the parameters (γ, γ_0, b or γ_∞).

The size of the dataset we chose (382 different accretion scenarios, spanning different core compositions, see Clesi & Deguen (2023)) also allows us to assess the sensitivity of the actual values within a formalism to the others parameters in the models. Indeed, the variations of T^{is}_{CMB}, as shown in Clesi & Deguen (2023), depend also on the composition of the core (light element concentrations), the pressure of equilibrium and its variation throughout accretion as well as the oxygen fugacity of the impactors. A small dispersion of the T^{is}_{CMB} values means that the Grüneisen parameter obtained for the set of parameter tends to mask the sensitivity of the model to other parameters (composition, pressure...). A large dispersion of T^{is}_{CMB} on the other hand means that the Grüneisen parameter tend to exacerbate the effect of the other parameters of the model.

As shown in the following sections, varying the values of the Grüneisen parameter can change the output of the same models by several hundreds of Kelvin. When modeling the compression of liquid metal, especially at high pressure, the data on compressibility is mostly derived from solid iron experiments and *ab initio* calculations. This situation presents several problems when modeling the Earth's core: the fact that liquid metal compressibility is not well constrained, and the fact that several light elements can affect this compressibility compared to pure iron. The Grüneisen parameter presents the advantage of having a limited range of value, thus extrapolating from solid iron value to the metal alloy forming the core limits the risk in terms of temperature calculation.

On the other hand, this advantage of having less chance to be far away from the results can become a disadvantage when trying to be more precise (for instance investigating the effect of small variations in composition on the temperature).

In the following sections we discuss the effect and robustness of the different formalisms presented above by using the sensitivity results obtained by fitting Equation 14 to the mean values of T^{is}_{CMB}. To do so we will estimate the variation of temperature induced by a deviation from the following values:

- in Section 3, a constant γ of 1.7, as used by Labrosse (2015) ;
- in section 4, Anderson (1967) formalism with $\gamma_0 = 2.05$ and $b = 0.63$ from Kuwayama et al. (2020);

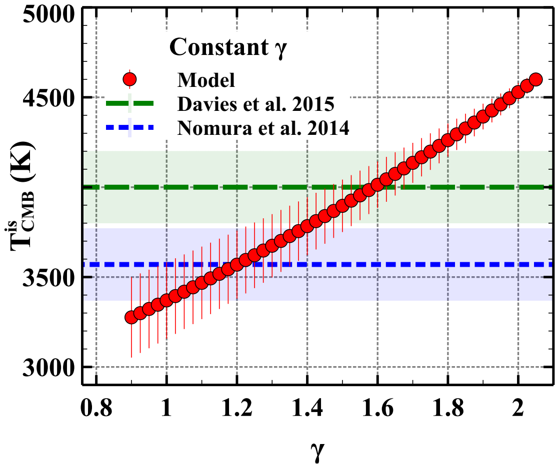

Figure 4. Variation of the mean T^{is}_{CMB} determined by Equations 8 and 9 as a function of γ. The error bar are the 2σ variation on the subset of core formation models used in this study. For comparison the estimates of current CMB temperature from Nomura et al. (2014) (dotted blue line) and Davies et al. (2015) (dashed green line) are also shown.

- in Section 5, Al'Tshuler et al. (1987) formalism with $\gamma_0 = 1.875$ and $\gamma_\infty = 1.305$ from Clesi & Deguen (2023).

3 CONSTANT GAMMA

Figure 4 shows the effect of varying the value of a constant γ on the isentropic temperature at the CMB. The range of γ tested is between 0.9 and 2.1, which is representative of the range of values of γ for iron given by several authors (see Dubrovinsky et al. (2000) or Wagle & Steinle-Neumann (2019) and references therein). T^{is}_{CMB} is increasing with increasing γ: the mean value goes from 3424 K to 4615 K. The effect of γ on the mean CMB temperature can be fitted by a polynomial function, for which the parameters are given in Table 2.

The 2σ values are higher as γ decreases: from 440 K at $\gamma = 0.9$ to 60 K at $\gamma = 2.05$. This

a_0	a_1	χ^2
2116	1202	1.6676

Table 2. Values of parameters fitting the trend of mean values in Figure 4. The equation fitted is Equation 14 with x replaced by γ.

indicates that the variability coming for the different accretion histories is buffered by high values of γ.

From Table 2, it is possible to calculate the ΔT (error on the final temperature at the CMB) induced by changing the value of γ from a reference value chosen to be $\gamma = 1.7$. With the value of a_1 from Table 2, changing γ by ± 0.1 induces a variation $\Delta T = 120$ K, which is higher than the dispersion of values observed in the other formalisms tested in this study. This trend shows that the results are highly sensitive to the value of a constant γ.

4 ANDERSON'S POWER LAW

The formalism of Anderson (1967) has two parameters that can affect the sensitivity of T^{is}_{CMB} to γ. The parameter b values are empirically fitted for each composition of the metal, with values spanning from 0.63 (Kuwayama et al. 2020) and 0.69 (Dubrovinsky et al. 2000) to 1.0 (McQueen et al. 1970) and 1.69 (Jeanloz 1979). In the case of liquid metal, most of the values converges toward $b \leq 1$. Here we tested values of b between 0.4 and 1.1 so as to cover the entire range of b values obtained from the fitting of Murphy et al. (2011)'s data set (see Table 1). As for the γ_0 value, it is the value for liquid metal at 1 bar, and since γ decreases with pressure it has to be higher than the value of γ at high pressures. The published range for γ_0 is between 1.59 (Brown & McQueen 1986) and 2.05 (Kuwayama et al. 2020), with 1.713 (Anderson & Ahrens 1994) and 1.8 (Dubrovinsky et al. 2000) having also been proposed and used. As for the value of b, we tested the range presented in Table 1, which is 1.5 to 2.2.

The top panel of Figure 5 shows that increasing the value of γ_0 tends to increase the mean value of T^{is}_{CMB}, irrespectively of the value of b. For $\gamma_0 = 1.2$, the mean value of T^{is}_{CMB} is between 3227 K and 3492 K, and for $\gamma_0 = 2.1$ the mean value is between 3869 K and 4474 K, depending on the value of b. ; for $b = 1.1$, the temperature varies between 4131 and 3500 K over the same γ_0 range. The sensitivity of T^{is}_{CMB} to γ_0 is stronger at the lower values of b, though this effect is not very strong. The bottom panel of Figure 5 shows the effect of increasing the exponent of the power law. The higher b is, the lower the temperature is: for $b = 0.4$ the temperature is between 4535 K and 3750 K depending on γ_0 values; for $b = 1.1$ the mean value is between 3527 K and

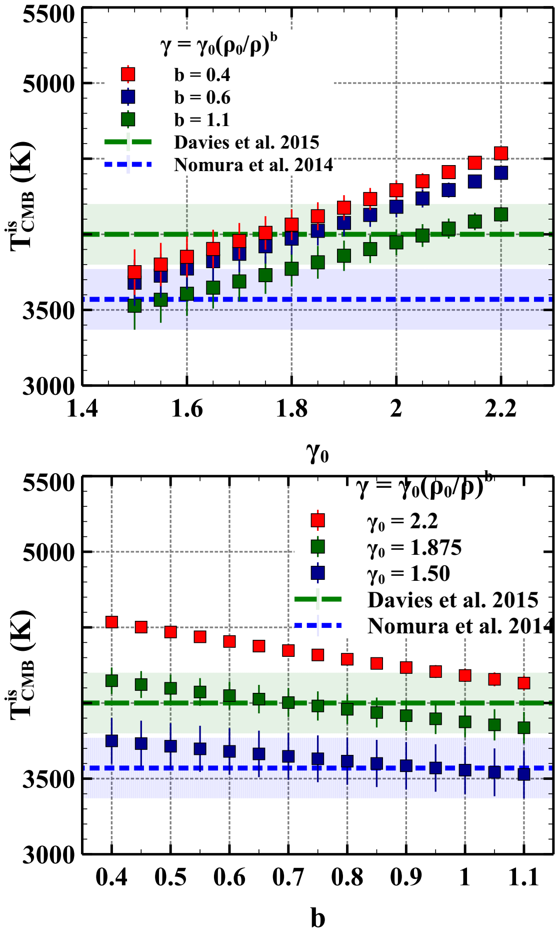

Figure 5. Top Panel: Effect of γ_0 on T^{is}_{CMB} for different values of b. Red squares: $b = 0.4$. Dark blue squares: $b = 0.6$. Dark green squares: $b = 1.1$.

Bottom panel: Effect of b on T^{is}_{CMB} for different values of γ_0. Red squares: $\gamma_0 = 2.2$. Dark green squares: $\gamma_0 = 1.875$. Dark blue squares: $\gamma_0 = 1.5$.

T^{is}_{CMB} is calculated from equations 8 and 11. For comparison, we also show the estimates of present-day CMB temperature from Nomura et al. (2014) (dotted blue line, lower estimate) and the review of Davies et al. (2015) (dashed green line).

4131 K. The higher the value of γ_0 and the lower the value of b, the lower the dispersion of values: for $b = 0.4$, the 2σ variation is 22 K at $\gamma_0 = 2.2$ and 150 K at $\gamma_0 = 1.5$; for $b = 1.1$ the 2σ is 48 K and 160 K for $\gamma_0 = 2.2$ and $\gamma_0 = 1.5$ respectively.

A linear fit (Equation 14) of the effect of both parameters on the mean values can be performed with good χ^2 values. The fitted parameter are shown in Table 3, showing a positive effect of γ_0, and a negative effect of b.

Let us now assume that we used the values of $\gamma_0 = 2.05$ and $b = 0.6$ from Kuwayama et al.

Conditions	a_0	a_1	χ^2
$b = 0.4$	1984	1158	0.1855
$b = 0.6$	2059	1065	0.1151
$b = 1.1$	2197	877	0.0424
$\gamma_0 = 2.2$	4764	-587	0.4068
$\gamma_0 = 1.875$	4319	-445	0.0244
$\gamma_0 = 1.5$	3872	-317	0.0041

Table 3. Values of parameter fitting the trend of mean values in Figure 5. The equations fitted are: $\overline{T^{is}_{CMB}} = a_0 + a_0\gamma_0$, and $\overline{T^{is}_{CMB}} = a_0 + a_1 b$. The first part of the table shows the variation for fixed values of b (Figure 5 left panel), and the second part shows the variation for fixed values of γ_0 (Figure 5 right panel).

(2020) to make the calculation on the models of Clesi & Deguen (2023). It is then possible to use the parameters from table 3 to calculate what is the induced error if the 'true' values are different. For $\gamma_0 = 2.2$, changing b by only 0.1 (corresponding to 15$\%$ of the range of values given in Table 1) changes T^{is}_{CMB} by 58 K. If we rather consider $b = 0.6$, then a variation of 0.1 (also corresponding to 15$\%$ of the range of values given in Table 1) for the parameter γ_0 yields $\Delta T \sim 100$ K.

The error induced by getting a wrong value for the exponent is therefore less important than getting the value of γ_0 wrong, but the variations are not negligible, especially if both parameters estimations are wrong: if for example $\gamma_0 = 1.875$ and $b = 0.4$, then the final temperature calculated with the reference values ($\gamma_0 = 2.05$ and $b = 0.6$) is overestimated by ~ 300 K.

5 AL'TSHULER POWER LAW

The formalism of Al'Tshuler et al. (1987) depends on two parameters, γ_0 and γ_∞, with $\gamma_\infty < \gamma_0$. The values of γ_∞ represent the minimum value of the Grüneisen parameter for infinite pressure (i.e. when the compressibility reaches a minimum asymptotic value) due to the quantum-statistical Grüneisen coefficient under extreme pressure (Gilvarry 1956; Burakovsky & Preston 2004). For liquid iron this value is between 1 and 1.4 (Dewaele et al. (2006), and references therein), and we tested values between 0.6 and 1.25 as given in Table 1. As for γ_0, it is the value of the Grüneisen parameter at the pressure of the reference state ($\rho/\rho_0 = 1$). Therefore it is higher than γ_∞ and

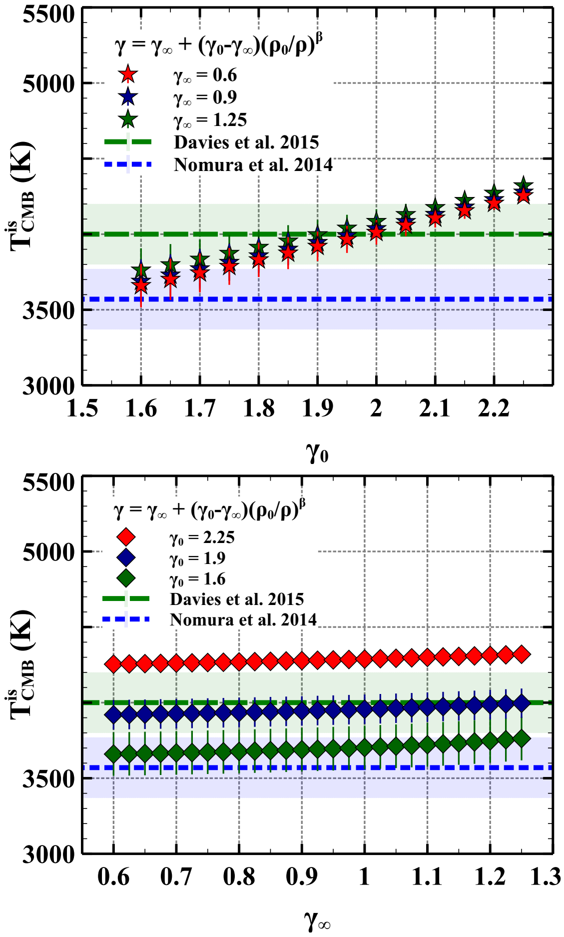

Figure 6. Evolution of the mean value of T^{is}_{CMB} as a function of γ_0 (top) and γ_∞ (bottom) in the formalism of Al'Tshuler et al. (1987), given by equations 13 and 8. On the top panel γ_∞ values are fixed at 1, 1.25, 1.305 and 1.5. On the bottom panel, γ_0 values are fixed at 2.05, 1.875, 1.75 and 1.5. For comparison we also show the estimates of current CMB temperature from Nomura et al. (2014) (dotted blue line) and Davies et al. (2015) (dashed green line).

close to the values of the parameter γ_0 from Anderson (1967), studied in the previous section. Here we tested values between 1.6 and 2.25, as given by the results of the fit in Table 1. Figure 6 shows that the temperature is positively correlated with both γ_0 and γ_∞. Higher values of γ_0 lead to less dispersion of the results: for instance, at $\gamma_\infty = 0.6$, the 2σ value for the dataset is 35 K for $\gamma_0 = 2.25$ and 144 K for $\gamma_0 = 1.6$. When γ_0 is fixed, varying the value of γ_∞ has less impact on the dispersion of the results: for instance at $\gamma_0 = 1.6$, the 2σ for the dataset is 141 K for $\gamma_\infty = 0.9$ and 128 K for $\gamma_\infty = 1.25$.

The variation of the mean temperature of our dataset is more affected by varying γ_0 than γ_∞. For instance, the mean temperature goes from 4319 K to 3762 K with $\gamma_\infty = 1.25$ and for γ_0

Conditions	a_0	a_1 χ^2	
$\gamma_0 = 2.25$	4191	100	0.0047
$\gamma_0 = 1.9$	3845	115	0.0013
$\gamma_0 = 1.6$	3560	150	0.0020
$\gamma_\infty = 0.6$	2151	933	0.0538
$\gamma_\infty = 0.9$	2188	927	0.0629
$\gamma_\infty = 1.25$	2312	890	0.1284

Table 4. Values of parameters fitting the trend of mean values in Figure 6. The equation fitted is: $\overline{T^{is}_{CMB}} = a_0 + a_1\gamma_x$, with γ_x being γ_0 or γ_∞. The first part of the table are for fixed values of γ_∞, the second one for fixed values of γ_0. The value of χ^2 for each fit is given in the last column.

varying from 2.25 to 1.6, respectively. On the other hand the temperature decreases from 4319 K to 4254 K with $\gamma_0 = 2.25$ for γ_∞ varying from 1.25 to 0.6, respectively.

The linear fits of the mean values of T^{is}_{CMB} yield good χ^2 values, with the parameters values given in Table 4. T^{is}_{CMB} correlates positively with both γ_0 and γ_∞, and the strongest effect of γ_0 is due to the higher value of a_1 (Table 4).

The variations in temperature are minimized if $\gamma_0 \geq 2$ and $\gamma_\infty \leq 1$, as shown by the corresponding values of the fit in Table 4. Therefore, choosing high values of γ_0 (like 1.837 as in Dewaele et al. (2006) and Clesi & Deguen (2023) or 2.05 as in Kuwayama et al. (2020)) combined with relatively low values of γ_∞ can minimize the error in the output. The γ_∞ value of 1.3 used in Dewaele et al. (2006) and Clesi & Deguen (2023) or 1.2 for Dubrovinsky et al. (2000) are a bit high in terms of minimizing the dispersion and error in the output.

Let us now assume that the values of $\gamma_0 = 1.875$ and $\gamma_\infty = 1.305$ in the original study of Clesi & Deguen (2023) (taken from Dewaele et al. (2006)) are wrong. It is then possible to estimate the error induced in the final mean temperature by calculating the variation in temperature induced by a variation in the values of γ_0 and γ_∞ using the parameters in Table 4. For $\gamma_0 = 1.875$, a variation in γ_∞ value by 0.1 induces a variation of the temperature of ~ 15 K. The main parameter that can induce error is γ_0: for $\gamma_\infty = 1.25$, a deviation of ± 0.1 in the value of γ_0 leads to a deviation of ~ 90 K. Then if the value of γ_0 is not the one proposed by Dewaele et al. (2006), but the one proposed by Kuwayama et al. (2020) ($\gamma_0 = 2.05$), even if the value of γ_∞ is correct, then ΔT would be a positive 200K, meaning that the initial value from Clesi & Deguen (2023) underestimates the temperature. Getting the value wrong would place the conclusions of the study towards a conservative estimate of the temperature.

6 DISCUSSION

We propose in the previous sections an overview of the effect of each parameter on the output of a given model. All three formalisms have their own merits and none of them should be discarded *a priori*. In this section we will provide an estimate of the error induced by the type and values used in each formalism, and argue that one can choose the formalism that suits the best the purpose of the study.

6.1 Thermodynamical theory compliance vs practicality

In terms of theoretical merits, Al'Tshuler et al. (1987) is the more correct formalism. It is derived from the study of variations in isotherms using the original definition of the parameter of Grüneisen (1912), and Mie-Gruneisen equation of state. The whole original paper of Al'Tshuler et al. (1987), is very strong in terms of theoretical compliance, since the relationship between density and Grüneisen parameter is derived by calculus alone. It also takes into account the asymptotic behavior of γ at high pressure (Burakovsky & Preston 2004). On the other hand, the formalism of Anderson (1967) is justified only by the sentence:

"*Assuming the power law* $\gamma = \gamma_0 \left(V/V_0\right)^q$"

followed by an integration of the γ function. In term of theoretical soundness, it is less sound than Al'Tshuler et al. (1987) study. But in term of integration and data fitting, it is more convenient. Indeed, this formalism combined with a Murnaghan equation of state yield an easy-to-integrate formula, while still fitting the experimental data.

The same kind of reasoning applies for studies using constant γ, despite its limitations. Table 2 shows that the variations in temperature induced by a choice of constant value are much larger. Furthermore, there is extensive experimental (Boehler & Ramakrishnan 1980; Dubrovinsky et al.

	Absolute ΔT (K)	Relative ΔT (%)
Mean	3.21	0.08
Minimum	0.008	0.0001
Maximum	8.05	0.20

Table 5. Difference ΔT between the core temperature T_{CMB}^{is} obtained using Anderson's and Al'Tshuler's power laws with the mean values of the parameters given in Table 1. The table gives the mean difference amongst our core-formation models (Clesi & Deguen 2023), as well as the minimum and maximum of ΔT. The formalism of Al'Tshuler is the reference point for calculating the relative variation in temperature

2000) and theoretical (Gilvarry 1956; Al'Tshuler et al. 1987) evidences that the Grüneisen parameter is not independent of pressure. However, the integration of a constant parameter within a much more complicated model tends to simplify readability and interpretations. One example is the study of the energetics of the core (*e.g.*Labrosse 2015): γ is not expected to vary strongly within the core, and the effect of these variations is likely secondary compared to the effect of thermal conductivity variations.

6.2 Assessing the uncertainties in the output of the model

Using the dataset of Murphy et al. (2011), we fitted the range of plausible value for each parameter in the formalism of Anderson (1967) and Al'Tshuler et al. (1987). This allows us to assess the error induced by choosing one formalism over another, and the error induced by choosing a parameter value over another in a given formalism. When using the mean value presented in Table 1 in each formalism, we can compare the effect of choosing one formalism over another by calculating, for each model in the dataset, the difference in T_{CMB}^{is}. In Table 5, we show the results of this comparison with $\Delta T = T_{CMB}^{is}(Anderson) - T_{CMB}^{is}(Al'Tshuler)$. The formalism of Anderson tends to yield higher values of T_{CMB}^{is} in any case, but the difference is small (8 K, 0.2% of variation maximum). Therefore, as long as the parameters of each formalism are consistently fitted to the same dataset, choosing a formalism does not induce much variations. On the other hand, the range of values chosen within a formalism is much more important than the variations induced by a chosen formalism. In Table 6 we show the range of variation when using the maximum and minimum values of the parameters presented in Table 1. Variation in the values of γ_0 is the most

	Mean ΔT	Minimum ΔT	Maximum ΔT
$\gamma_0 = 1.555$	-300 K (-7.56%)	-226 K (-5.47%)	-334 K (- 8.52%)
$\gamma_0 = 2.195$	331.5 K (8.34%)	243 K (5.90%)	372 K (9.49%)
$b = 0.432$	152 K (3.8%)	136 K (3.30%)	156 (3.98%)
$b = 1.07$	-132 K (8.34&)	-118 K (5.89%)	-136 K (9.48%)
$\gamma_0 = 1.608$	-279 K (-7.03%)	-205 K (-4.98%)	-313 K (-7.99%)
$\gamma_0 = 2.258$	311 K (7.83%)	223 K (5.43%)	351 K (8.97%)
$\gamma_\infty = 0.591$	-27.15 K (-0.68%)	-26 K (-0.64%)	-27 K (-0.70%)
$\gamma_\infty = 1.241$	47 K (1.17%)	45 K (1.09%)	47 K (1.19%)

Table 6. Variation of ΔT within a chosen formalism. The absolute value are in K, the number in parenthesis are the variation relatively to the mean value in %. Top part of the Table: Anderson's power law parameter. Bottom part: Al'Tshuler power law parameter. The variation on temperature is calculated using the temperature obtained by calculating with the mean value of the parameter presented in Table 1. The terms maximum and minimum refers to the absolute deviation from the initial value, not to the value itself (i.e -205 K is a higher value than -313 K but the absolute variation is lower) .

important: the mean variation induced by a change in γ_0 value in both formalisms yield a mean ΔT of ~ 300 K, slightly lower in the Al'Tshuler formalism (Table 6). Varying the parameter γ_∞ within the range given in table 1 yield a low error range, between -26 K and $+50$ K (Table 6). On the other hand, the range of b values given in Table 1 yield variations of temperature between -136 K and $+156$ K. The Anderson formalism is more prone to yielding large error: taking into account both parameters value ranges, the final value of T^{is}_{CMB} can vary by $\sim 20\%$, with a mean variation of $11 - 15\%$. The range of T^{is}_{CMB} is smaller when using Al'Tshuler formalism: given the small variation induced by an error on γ_∞, the maximum error on the final value of T^{is}_{CMB} is $\sim 10\%$, with a mean error of $\sim 8\%$. In summary, the Al'Tshuler formalism yield lower uncertainties than the Anderson formalism on this type of model. However, when fitting any of the formalism to the same dataset, there is little to none variation in the output (Table 5). Since, as it is done in this study, it is possible to explain satisfactorily the same data with two different formalisms, the choice of formalism is not critical. For instance the data of Boehler & Ramakrishnan (1980) is fitted with Anderson (1967) formalism, but is used by Al'Tshuler et al. (1987) to test the formalism. The two formalisms are close in terms of mathematical writing (both of them are power laws) so it may be that for a given problem and a given dataset of γ values, either formalism can be used (with different values of parameters). In this instance it depends on the quality of the data available and the best fit available. This problem of uncertainties range and representativity of the data needs to be addressed when choosing a formalism and the values of parameters.

6.3 Choosing a formalism and its parameter value: a function of the study's goal

In the original study of Clesi & Deguen (2023) the choice has been made to use the formalism of Al'Tshuler et al. (1987) with the values of Dewaele et al. (2006). In the supplementary information of the same study are presented different results with the Grüneisen parameter formalism of Anderson (1967) with the values of Kuwayama et al. (2020). The results are sensibly different with everything else being the equal. In this section we argue that, for this particular type of model, it is indeed better to use Al'Tshuler et al. (1987) formalism, because it enhances the robustness and replicability of the results. Indeed, using Al'Tshuler formalism is limiting the variance and the risk of error, as shown previously in Section 5, and limits the overall uncertainty of the result as shown in Section 6.2. Furthermore, in the models presented in Clesi & Deguen (2023) and briefly re-explained in section 2.1, there are several hypotheses that are made and are a source of possible error in the model; among others: the number of element in the compositional model, the equilibrium rate, the discretization of core/mantle segregation in 20 steps, the choice of equation of state, the parameters values of equation of state, the neglect of dissipation and diffusion, the thermal state of the solid mantle... All of these hypotheses are more accurately described and justified in the original publication. On top of these simplifying hypotheses, the values of γ_0 and γ_∞ from Dewaele et al. (2006) are assumed to be independent of the composition of the core, which might be a source of error in the model. Choosing a robust formalism that limits the variation if those values are wrong is then a better option: for instance the main purpose of the publication of Clesi & Deguen (2023) is to show the existence of a correlation between core composition and its temperature, doing so by applying a number of hypotheses, which is a broader goal than getting a precise value for the core temperature. Thus, limiting the scattering of the results when many other process in the model might also be a source of scattering helps us to get a better view of the problem. After all, for models of this type, it may be hard to tell if the scattering of the results is an actual scattering or an artifact created by the hypotheses and calculations techniques. This kind of limitation in the scattering also facilitates comparison between studies. For instance, one topic that is highly debated is the amount of light elements such as N, H or C in the core (Malavergne et al. 2019; Grewal et al. 2019; Fischer et al. 2020; Blanchard et al. 2022; Suer et al. 2023). The presence of such elements in the core will affect the temperature of the core by affecting the density of the metal, which in turn affects the temperature (through the effect of density on γ; see Equations 2, 7 and 8. However, each of the aforementioned study use a different model of accretion with a different set of hypothesis than in the Clesi & Deguen (2023). If one were to calculate the effect of carbon on temperature using the data and accretion models of Fischer et al. (2020) or Blanchard et al. (2022) studies in combination with a thermal evolution model, and find a significant effect of the carbon concentration on the temperature, can this effect be attributed to carbon or to the type of accretion and thermal model used to calculate carbon concentration and temperature? Among the source of uncertainties is the Grüneisen parameter formalism and value. Using a less sensitive formalism such as Al'Tshuler will at least close one of the point of discussion about the validity of the results: whether or not the values of γ_0 and γ_∞ are the 'true' values, at least the error is low and if differences arise between models, then they are probably not due to the Grüneisen parameter. On the other hand, if the end goal is to best describe the entirety of the phenomenon or get a precise estimate of the core temperature (Driscoll & Davies 2023; Dobrosavljevic et al. 2022), then the best formalism is the one that fits the best the data, or the values that are calculated directly within *ab initio* studies (Vočadlo 2007; Alfè 2009; Alfè et al. 2007). If one would use a core segregation model to calculate the actual temperature at the CMB instead of highlighting the correlations between parameters, or actually deriving a precise value on those correlations, then the choice of formalism and parameters value must be driven by the quality of the data, the quality of the fit, and the range of uncertainties on the parameters as highlighted in section 6.2. As an example, let us assume one wants to calculate the effect of hydrogen incorporation in the core on temperature using for instance models from Clesi et al. (2018), Malavergne et al. (2019) or Suer et al. (2023). There are some data available on the hydrogen effect on the Grüneisen parameter (Umemoto &

Hirose 2015). If Anderson's formalism fitted to the data from Umemoto & Hirose (2015) yields a narrower range of value for γ_0 and b, than the range of value for γ_0 and γ_∞ obtained through fitting the data with Al'Tshuler formalism, then using the formalism of Anderson would be better, especially if the range is narrow enough to yield smaller error than the one presented in Table 6.

6.4 Implications for the CMB temperature

As highlighted in the previous sections, there are some limitations to the inferences that can be made yet as to the relationship between the Grünesien parameter and the core temperature. The main goal of this study is to derive the sensitivity of T^{is}_{CMB} to the variations of parameters controlling the Grüneisen parameter. However, from the sensitivity study some implications can be drawn about the initial temperature of the core.

All three formalisms applied to the model described in Section 2.1 can yield acceptable T^{is}_{CMB} for the Earth when compared to current estimates of CMB temperature from Zhang et al. (2016) or Davies et al. (2015) ($4000 \pm 200K$), Nomura et al. (2014) ($3570 \pm 200K$) or Dobrosavljevic et al. (2022) ($3500{\pm}200K$). In all the formalisms presented, it is possible to find values of the parameters that yield initial T^{is}_{CMB} higher than the current estimates listed above. However, none of the values tested and presented in Figures 4, 5 and 6 can yield initial temperature at the CMB compatible with the estimates of Andrault et al. (2017) (5400 ± 100 K) or Driscoll & Davies (2023) (5000 to 6000 K). This may be due to the own limitations of the model used in this study. Indeed, among other limitations described in the orignal paper (Clesi & Deguen 2023), the viscous dissipation that tends to increase temperature of the core (King & Olson 2011) is neglected, thus leading to lower temperatures. Furthermore the choice of the Murnaghan equation of state to simplify the calculations can also lead to an underestimation of temperature. This does show the importance of having constraints on this parameter when trying to constrain the core temperature precisely.

7 CONCLUSION

The Grüneisen parameter γ is an important parameter when studying the thermal state of the core, yet its value is not very well known for different composition of iron alloys in the core. Different formalisms are used throughout the litterature: constant values, *ad hoc* power law (Anderson 1967) and thermodynamically derived power law (Al'Tshuler et al. 1987). With this sensitivity study, we show that the thermodynamically derived power law of Al'Tshuler et al. (1987) is less likely to yield errors when the actual values of the parameters controlling γ are not precisely known, and is theoretically more sound than the *ad hoc* power law of Anderson (1967).

However, with the data at hand it is not yet possible to exclude any formalism or parameter values based on this study alone. Nonetheless, the sensitivity of temperature to the Grüneisen parameter can be high depending on the formalism adopted and need to be acknowledged when modeling temperature evolution. Further work in constraining the compositional dependencies of the parameters would greatly improve the thermal models of the core and their links to the light element concentrations.

ACKNOWLEDGMENT

This work was supported by the European Research Council (ERC) under the European Unions Horizon 2020 research and innovation programme (grant number 716429). ISTerre is part of Labex OSUG@2020 (ANR10 LABX56). The authors declare no other sources of funding and no competing interest.

Data availability

The code and data will be made available upon demand to the corresponding author.

REFERENCES

Alfè, D., Gillan, M., & Price, G., 2007. Temperature and composition of the earth's core, *Contemporary Physics*, **48**(2), 63–80.

Alfè, D., 2009. Temperature of the inner-core boundary of the Earth: Melting of iron at high pressure from first-principles coexistence simulations, *Physical Review B*, **79**(6), 060101.

Al'Tshuler, L., Brusnikin, S., & Kuz'Menkov, E., 1987. Isotherms and Grüneisen functions for 25 metals, *Journal of Applied Mechanics and Technical Physics*, **28**(1), 129–141.

Anderson, O. L., 1967. Equation for thermal expansivity in planetary interiors, *Journal of Geophysical Research*, **72**(14), 3661–3668.

Anderson, W. W. & Ahrens, T. J., 1994. An equation of state for liquid iron and implications for the Earth's core, *Journal of Geophysical Research: Solid Earth*, **99**(B3), 4273–4284.

Andrault, D., Bolfan-Casanova, N., Nigro, G. L., Bouhifd, M. A., Garbarino, G., & Mezouar, M., 2011. Solidus and liquidus profiles of chondritic mantle: Implication for melting of the Earth across its history, *Earth and planetary science letters*, **304**(1-2), 251–259.

Andrault, D., Bolfan-Casanova, N., Bouhifd, M., Boujibar, A., Garbarino, G., Manthilake, G., Mezouar, M., Monteux, J., Parisiades, P., & Pesce, G., 2017. Toward a coherent model for the melting behavior of the deep earth's mantle, *Physics of the Earth and Planetary Interiors*, **265**, 67–81.

Badro, J., Côté, A. S., & Brodholt, J. P., 2014. A seismologically consistent compositional model of earth's core, *Proceedings of the National Academy of Sciences*, **111**(21), 7542–7545.

Blanchard, I., Rubie, D.C., Jennings, E.S., Franchi, I.A., Zhao, X., Petitgirard, S., Miyajima, N., Jacobson, S.A. & Morbidelli, A., 2022. The metal–silicate partitioning of carbon during earth's accretion and its distribution in the early solar system, *Earth and Planetary Science Letters*, **580**, 117374.

Boehler, R. & Ramakrishnan, J., 1980. Experimental results on the pressure dependence of the grüneisen parameter: A review, *Journal of Geophysical Research: Solid Earth*, **85**(B12), 6996–7002.

Bouffard, M., Landeau, M., & Goument, A., 2020. Convective erosion of a primordial stratification atop Earth's core, *Geophysical Research Letters*, **47**(14), e2020GL087109.

Brown, J. M. & McQueen, R. G., 1986. Phase transitions, Grüneisen parameter, and elasticity for shocked iron between 77 GPa and 400 GPa, *Journal of Geophysical Research: Solid Earth*, **91**(B7), 7485–749.

Burakovsky, L. & Preston, D. L., 2004. Analytic model of the grüneisen parameter all densities, *Journal of Physics and Chemistry of Solids*, **65**(8-9), 1581–1587.

Clesi, V., Bouhifd, M. A., Bolfan-Casanova, N., Manthilake, G., Schiavi, F., Raepsaet, C., Bureau, H., Khodja, H., & Andrault, D., 2018. Low hydrogen contents in the cores of terrestrial planets, *Science advances*, **4**(3), e1701876.

Clesi, V. & Deguen, R., 2023. Linking the core heat content to earth's accretion history, *Geochemistry, Geophysics, Geosystems*, **24**(5), e2022GC010661.

Davies, C., Pozzo, M., Gubbins, D. & Alfe, D., 2015. Constraints from material properties on the dynamics and evolution of Earth's core, *Nature Geoscience*, **8**(9), 678–685.

Dewaele, A., Loubeyre, P., Occelli, F., Mezouar, M., Dorogokupets, P. I., & Torrent, M., 2006. Quasihydrostatic equation of state of iron above 2 Mbar, *Physical Review Letters*, **97**(21), 215504.

Dobrosavljevic, V. V., Zhang, D., Sturhahn, W., Zhao, J., Toellner, T. S., Chariton, S., Prakapenka, V. B., Pardo, O. S., & Jackson, J. M., 2022. Melting and phase relations of fe-ni-si determined by a multi-technique approach, *Earth and Planetary Science Letters*, **584**, 117358.

Driscoll, P. & Davies, C., 2023. The "new core paradox:" challenges and potential solutions, *Journal of Geophysical Research: Solid Earth*, p. e2022JB025355.

Dubrovinsky, L., Saxena, S., Dubrovinskaia, N., Rekhi, S., & Le Bihan, T., 2000. Gruneisen parameter of ε-iron up to 300 GPa from in-situ X-ray study, *American Mineralogist*, **85**(2), 386–389.

Fischer, R. A., Cottrell, E., Hauri, E., Lee, K. K., & Le Voyer, M., 2020. The carbon content of earth and its core, *Proceedings of the National Academy of Sciences*, **117**(16), 8743–8749.

Gilvarry, J. J., 1956. Grüneisen's law and the fusion curve at high pressure, *Physical Review*, **102**(2), 317.

Gomi, H., Ohta, K., Hirose, K., Labrosse, S., Caracas, R., Verstraete, M. J., & Hernlund, J. W., 2013. The high conductivity of iron and thermal evolution of the earth's core, *Physics of the Earth and Planetary Interiors*, **224**, 88–103.

Grewal, D.S., Dasgupta, R., Sun, C., Tsuno, K., & Costin, G., 2019. Delivery of carbon, nitrogen, and sulfur to the silicate Earth by a giant impact, *Science advances*, **5**(1), eaau3669.

Grüneisen, E., 1912. Theorie des festen zustandes einatomiger elemente, *Annalen der Physik*, **344**(12), 257–306.

Hirose, K., Labrosse, S., & Hernlund, J., 2013. Composition and state of the core, *Annual Review of Earth and Planetary Sciences*, **41**, 657–691.

Hsieh, W.-P., Goncharov, A. F., Labrosse, S., Holtgrewe, N., Lobanov, S. S., Chuvashova, I., Deschamps, F., & Lin, J.-F., 2020. Low thermal conductivity of iron-silicon alloys at earth's core conditions with implications for the geodynamo, *Nature communications*, **11**(1), 3332.

Ichikawa, H., Tsuchiya, T. & Tange, Y., 2014. The P-V-T equation of state and thermodynamic properties of liquid iron, *Journal of Geophysical Research: Solid Earth*, **119**(1), 240–252.

Jacobson, S. A., Rubie, D. C., Hernlund, J., Morbidelli, A., & Nakajima, M., 2017. Formation, stratification, and mixing of the cores of Earth and Venus, *Earth and Planetary Science Letters*, **474**, 375–386.

Jeanloz, R., 1979. Properties of iron at high pressures and the state of the core, *Journal of Geophysical Research: Solid Earth*, **84**(B11), 6059–6069.

King, C.& Olson, P., 2011 Heat partitioning in metal-silicate plumes during Earth d, *Earth and Planetary Science Letters*, **304**(3-4), 577–586.

Kuwayama, Y., Morard, G., Nakajima, Y., Hirose, K., Baron, A. Q., Kawaguchi, S. I., Tsuchiya, T., Ishikawa, D., Hirao, N., & Ohishi, Y., 2020. Equation of state of liquid iron under extreme conditions, *Physical Review Letters*, **124**(16), 165701.

Labrosse, S., 2015. Thermal evolution of the core with a high thermal conductivity, *Physics of the Earth and Planetary Interiors*, **247**, 36–55.

Landeau, M., Olson, P., Deguen, R., & Hirsh, B. H., 2016. Core merging and stratification following giant impact, *Nature Geoscience*, **9**(10), 786–789.

Landeau, M., Fournier, A., Nataf, H.-C., Cébron, D., & Schaeffer, N., 2022. Sustaining earth's magnetic dynamo, *Nature Reviews Earth & Environment*, **3**(4), 255–269.

Lin, J.-F., Campbell, A. J., Heinz, D. L., & Shen, G., 2003. Static compression of iron-silicon alloys: Implications for silicon in the earth's core, *Journal of Geophysical Research: Solid Earth*, **108**(B1).

Malavergne, V., Bureau, H., Raepsaet, C., Gaillard, F., Poncet, M., Surble, S., Sifré, D., Shcheka, S., Fourdrin, C., Deldicque, D., et al., 2019. Experimental constraints on the fate of H and C during planetary core-mantle differentiation. Implications for the Earth, *Icarus*, **321**, 473–485.

McDonough, W. & Sun, S.-S., 1995. The composition of the Earth, *Chemical geology*, **120**(3-4), 223–253.

McQueen, R.G., Marsh, S.P., Taylor, J.W., Fritz, J.N. & Carter, WJ, 1970. The equation of state of solids from shock wave studies, *High velocity impact phenomena*, **293**, 294–417.

Murphy, C. A., Jackson, J. M., Sturhahn, W., &Chen, B. 2011. Grüneisen parameter of hcp-Fe to 171 GPa, *eophysical Research Letters*, **38(24)**, L24306.

Nomura, R., Hirose, K., Uesugi, K., Ohishi, Y., Tsuchiyama, A., Miyake, A., & Ueno, Y., 2014. Low core-mantle boundary temperature inferred from the solidus of pyrolite, *Science*, **343**(6170), 522–525.

Suer, T.-A., Jackson, C., Grewal, D. S., Dalou, C., & Lichtenberg, T., 2023 The distribution of volatile elements during rocky planet formation, *Frontiers in Earth Science*, **11**, 1159412.

Umemoto, K. & Hirose, K., 2015. Liquid iron-hydrogen alloys at outer core conditions by first-principles calculations, *Geophysical Research Letters*, **42**(18), 7513–7520.

Vočadlo, L, 2007. 2.05 Mineralogy of the Earth–The Earth's Core: Iron and Iron Alloys, *Treatise on Geophysics*, 91–220.

Wagle, F. & Steinle-Neumann, G., 2019. Liquid iron equation of state to the terapascal regime from ab initio simulations, *Journal of Geophysical Research: Solid Earth*, **124**(4), 3350–3364.

Zhang, D., Jackson, J. M., Zhao, J., Sturhahn, W., Alp, E. E., Hu, M. Y., Toellner, T. S., Murphy, C. A., & Prakapenka, V. B., 2016. Temperature of Earth's core constrained from melting of Fe and Fe0. 9Ni0. 1 at high pressures, *Earth and Planetary Science Letters*, **447**, 72–83.